Epidermal Integrin α3β1 Regulates Tumor-Derived Proteases BMP-1, Matrix Metalloprotease-9, and Matrix Metalloprotease-3

Whitney M. Longmate[1,4], Rakshitha Pandulal Miskin[2,4], Livingston Van De Water[1,2] and C. Michael DiPersio[1,3]

As the major cell surface receptors for the extracellular matrix, integrins regulate adhesion and migration and have been shown to drive tumor growth and progression. Previous studies showed that mice lacking integrin α3β1 in the epidermis fail to form skin tumors during two-step chemical tumorigenesis, indicating a protumorigenic role for α3β1. Furthermore, genetic ablation of α3β1 in established skin tumors caused their rapid regression, indicating an essential role in the maintenance of tumor growth. In this study, analysis of immortalized keratinocyte lines and their conditioned media support a role for α3β1 in regulating the expression of several extracellular proteases of the keratinocyte secretome, namely BMP-1, matrix metalloprotease (MMP)-9, and MMP-3. Moreover, immunofluorescence revealed reduced levels of each protease in α3β1-deficient tumors, and RNA in situ hybridization showed that their expression was correspondingly reduced in α3β1-deficient tumor cells in vivo. Bioinformatic analysis confirmed that the expression of *BMP1*, *MMP9*, and *MMP3* genes correlate with the expression of *ITGA3* (gene encoding the integrin α3 subunit) in human squamous cell carcinoma and that high *ITGA3* and *MMP3* associate with poor survival outcome in these patients. Overall, our findings identify α3β1 as a regulator of several proteases within the secretome of epidermal tumors and as a potential therapeutic target.

JID Innovations (2021);**1:**100017 doi:10.1016/j.xjidi.2021.100017

INTRODUCTION

Integrins are the major cell surface receptors for the extracellular matrix (ECM), regulating adhesion and migration (Hynes, 2002). Integrins that are expressed on tumor cells have critical roles in driving tumor growth and progression (Cooper and Giancotti, 2019; Hamidi and Ivaska, 2018). Important roles have been identified for the laminin-binding integrin, α3β1, in tumorigenesis, including in the regulation of the tumor cell secretome, as reviewed (Longmate, 2020; Subbaram and DiPersio, 2011). For example, the roles for epidermal α3β1 in skin tumorigenesis have been elucidated using the two-step model of tumorigenesis—one of the best-characterized mouse models to study the stepwise tumor growth and progression that recapitulate many features of human carcinogenesis (Abel et al., 2009). Briefly, topical treatment with the tumor initiator 7,12-dimethylbenz[*a*]-anthracene followed by repeated treatment over weeks with the tumor promoter 12-*O*-tetradecanoylphorbol-13-acetate induces benign skin tumors (i.e., papillomas), a proportion of which progress to squamous cell carcinoma (SCC) depending on the genetic background (Abel et al., 2009). Previous studies by our group and others have used this model to demonstrate that epidermal α3β1 is essential for skin tumor formation (Longmate et al., 2017; Sachs et al., 2012) and that it is also required for the maintenance of skin tumor growth (Longmate et al., 2021).

Several studies have revealed the important roles for epidermal α3β1 in the regulation of the keratinocyte (KC) secretome (He et al., 2018; Longmate et al., 2021; Ramovs et al., 2020) and in cross-talk to stromal cells within the tumor microenvironment (TME) (Longmate et al., 2021; Ramovs et al., 2020; Zheng et al., 2019). Extracellular proteases are major constituents of the secretome that contribute to the state of the ECM by mediating matrix degradation and remodeling (Bonnans et al., 2014), which is accomplished by altering ECM constituents and biophysical properties (Niland and Eble, 2020). Matrix metalloproteases (MMPs), in particular, are extracellular proteases that have a central role in

[1]*Department of Surgery, Albany Medical College, Albany, New York, USA;* [2]*The Department of Regenerative and Cancer Cell Biology, Albany Medical College, Albany, New York, USA; and* [3]*Department of Molecular and Cellular Physiology (MCP), Albany Medical College, Albany, New York, USA*

[4]*These authors contributed equally to this work.*

Correspondence: C. Michael DiPersio, Department of Surgery, Albany Medical College, Mail Code 8, Room MR-421, 47 New Scotland Avenue, Albany, New York 12208-3479, USA. E-mail: dipersm@amc.edu

Abbreviations: CM, conditioned medium; ECM, extracellular matrix; IMK, immortalized mouse keratinocyte; ISH, in situ hybridization; KC, keratinocyte; MK, mouse keratinocyte; MMP, matrix metalloprotease; SCC, squamous cell carcinoma; TME, tumor microenvironment; TMK, transformed mouse keratinocyte

Received 17 February 2021; revised 5 April 2021; accepted 14 April 2021; accepted manuscript published online 30 April 2021; corrected proof published online 29 May 2021

Cite this article as: JID Innovations 2021;1:100017

Table 1. Summary of MK Lines Used in This Study, Including Information on Methods of Immortalization and Transformation (Where Applicable)

MK Line	Immortalization Method	Transformation Method	Original Reference
MK	SV40 Large T antigen	none	DiPersio et al. (2000)
IMK	$p53^{-/-}$	none	Lamar et al. (2008)
TMK	$p53^{-/-}$	RasV12	Lamar et al. (2008)

Abbreviations: IMK, immortalized mouse keratinocyte; MK, mouse keratinocyte; SV40, simian virus 40; TMK, transformed mouse keratinocyte.
See the Materials and Methods section for further details.

regulating the TME (Niland and Eble, 2020), and MMPs are critically involved in all stages of cancer progression (Flores-Reséndiz et al., 2009; Gill and Parks, 2008). Indeed, the progression of cancer is dependent on the proteolytic action of MMPs on the ECM of the TME (Niland and Eble, 2020). MMP-9 has been previously shown to be α3β1 dependent in mouse KC (MK) lines immortalized with large T antigen (DiPersio et al., 2000), and MMP-9 is elevated in SCC and other skin cancers (Goździalska et al., 2016; Ruokolainen et al., 2004). Two other metalloproteases, BMP-1 and MMP-3, have been implicated in the poor prognoses of several cancers (Mehner et al., 2015; Rafi et al., 2021; Xiao et al., 2020). We previously showed that BMP-1 is α3β1 dependent in MKs in vitro and during murine wound healing in vivo (Longmate et al., 2018). Moreover, we identified MMP-3 as part of the α3β1-dependent MK secretome using mass spectrometry (Longmate et al., 2021), although we did not assess α3β1 dependence of MMP-3 expression in vitro or in vivo.

In this study, we aimed to investigate whether proteases MMP-9, MMP-3, and BMP-1 are α3β1 dependent in three independent immortalized (nontumorigenic) or transformed (tumorigenic) KC lines in vitro as well as in murine skin tumors in vivo. Whereas our previous studies were performed in large T antigen–immortalized, nontumorigenic MK cells, this study includes MK lines that were immortalized or transformed with genetic lesions that reflect common causal mutations in human SCC, namely the deletion of the p53 tumor suppressor (immortalized MK [IMK] cells) and expression of the *RasV12* oncogene (transformed MK [TMK] cells) (White et al., 2011). qPCR analysis of all the three KC lines confirmed that α3β1 promotes *Bmp1*, *Mmp9*, and *Mmp3* expression but not *Mmp2* expression, and immunoblot of the conditioned media (CMs) from these lines showed that this pattern of regulation is maintained at the level of protein secretion. Immunofluorescence revealed that the levels of BMP-1, MMP-9, and MMP-3 were reduced in α3β1-deficient skin tumors in vivo. Moreover, RNA in situ hybridization (ISH) confirmed that mRNA transcripts for *Bmp1*, *Mmp9*, and *Mmp3* were each reduced in α3β1-deficient tumor cells. Bioinformatic analysis revealed that the expression of the *BMP1*, *MMP9*, and *MMP3* genes correlate with the expression of *ITGA3*, the gene that encodes the integrin α3 subunit, in human SCC, validating the relevance of our models to human SCC. Furthermore, higher expression of *ITGA3* and *MMP3* were associated with poor survival outcomes in these patients. Overall, our findings identify α3β1 as a regulator of the KC protease secretome.

RESULTS

α3-Null MKs have reduced BMP-1, MMP-9, and MMP-3 gene expression and protein secretion

For our study, we utilized a panel of three different MK lines that we developed previously in our laboratory: MK cells were immortalized using simian virus 40 large T antigen (DiPersio et al., 2000), IMK cells were immortalized by *p53*-null mutation and are nontumorigenic (Lamar et al., 2008), TMK cells were generated by transforming IMK cells with the *RasV12* oncogene and are tumorigenic (Lamar et al., 2008) (Table 1). Each KC line was derived originally from either a wildtype (α3+) mouse or an α3-null, neonatal mouse (α3–).

qPCR analysis revealed that α3-null cells of all the three lines displayed significantly reduced levels of *Bmp1*, *Mmp9*, and *Mmp3* mRNA, indicating that integrin α3β1 induces their gene expression (Figure 1a). In contrast, *Mmp2* mRNA levels were either higher or not significantly different in α3-null cells (Figure 1a). The α3β1-dependent regulation of MMP-9 in the IMK and TMK lines confirms our previous report (Lamar et al., 2008). As confirmed by immunoblot of cell lysates, α3-null KCs of all the three lines have no detectable α3 protein, (Figure 1b).

Consistently, immunoblotting of CM showed reduced secretion of BMP-1, MMP-9, and MMP-3 proteins in the α3-null cells of each line compared with the CM from the corresponding α3-expressing control line (Figure 2a and b). Secreted MMP-2 levels were not significantly different, although they did trend upward in two of the α3-null lines (Figure 2a and b), consistent with the qPCR data (Figure 1a). As expected, cell-associated MMP-9 and MMP-3 were also α3β1 dependent, as determined by immunoblot of the cell lysates from the TMK lines (Figure 2c). Compared with α3-expressing TMKs, α3-null TMKs showed greatly reduced levels of activated, processed forms of MMP-9 and MMP-3, presumably on the cell surface (Figure 2c), reflecting what was observed in the CM (Figure 2a and b). The indicated bands for unprocessed and processed forms (Figure 2c) are consistent in size (kDa) with reported sizes of mouse MMP-9 and MMP-3 (De Groef et al., 2015; DiPersio et al., 2000). Collectively, these findings indicate that integrin α3β1 regulates a subset of the KC protease secretome in vitro that includes BMP-1, MMP-9, and MMP-3 and that this regulation occurs, at least in part, at the mRNA level.

Ablation of integrin α3β1 from skin tumors leads to reduced levels of tumor cell–derived BMP-1, MMP-9, and MMP-3

Next, we evaluated the in vivo levels of BMP-1, MMP-9, and MMP-3, each confirmed as α3β1 dependent in vitro, comparing the cutaneous tumor tissues that express or lack

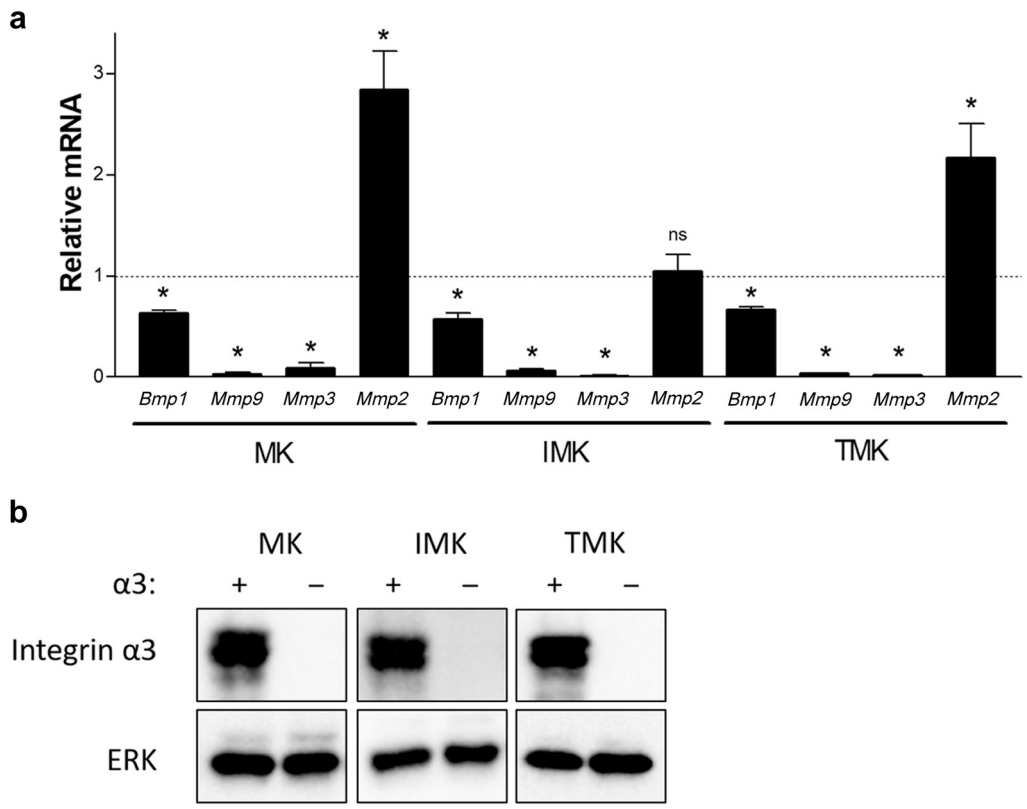

Figure 1. α3-Null cells have reduced *Bmp1, Mmp9,* and *Mmp3* gene expression. (**a**) qPCR analysis showing the relative *Bmp1* mRNA and MMP mRNAs, *Mmp9*, *Mmp3*, and *Mmp2*, in each of the MK cell lines. Bars represent the mRNA of α3-null cells normalized to that of their respective α3-expressing control (dotted line); n = 3. Data are presented as mean ± SEM; two-tailed *t*-test, $*P < 0.05$. (**b**) Whole-cell lysates from the keratinocyte panel were isolated and then assayed by immunoblot for the integrin α3 subunit or for total ERK as a loading control; representative immunoblots are shown. ERK, extracellular signal–regulated kinase; IMK, immortalized mouse keratinocyte; MK, mouse keratinocyte; MMP, matrix metalloprotease; ns, nonsignificant; TMK, transformed mouse keratinocyte.

epidermal α3β1. Constitutive ablation of α3β1 specifically in the epidermis, achieved through Cre-mediated deletion of floxed *Itga3* alleles (K14Cre:$\alpha3^{flx/flx}$), reduced both size and incidence of skin tumors that form in response to the two-step tumorigenesis protocol, demonstrating that α3β1 is essential for tumor formation (Longmate et al., 2017; Sachs et al., 2012). However, greatly reduced tumor formation in these mice prevented our ability to study α3β1-deficient tumor tissue. To generate tumor tissues that lack epidermal α3β1, we used K14CreERT:$\alpha3^{flx/flx}$ mice to gain temporal control over α3β1 deletion with tamoxifen (4-hydroxytamoxifen)-inducible Cre recombination. Briefly, papillomas were formed on the back skin of K14CreERT:$\alpha3^{flx/flx}$ mice using the two-step tumorigenesis protocol (see Materials and Methods section). As we have described previously, topical treatment with 4-hydroxytamoxifen after papilloma formation caused the deletion of the floxed *α3* gene, generating epidermal α3β1-deficient papillomas, whereas the vehicle-treated papillomas served as controls (Longmate et al., 2021). Consistent with our in vitro findings, immunofluorescence showed reduced levels of BMP-1, MMP-9, and MMP-3 protein in epidermal α3β1-deficient tumors (Figure 3).

Interestingly, we observed variation in the distributions of these three proteases within the tumors. BMP-1 appeared concentrated at the tumor–stroma border (Figure 3), consistent with the findings of our previous study that revealed a role for BMP-1 in laminin-γ2 chain processing at the epidermal–dermal junction (Longmate et al., 2018). In contrast, MMP-9 and MMP-3 were detected mainly in the tumor stroma (Figure 3), possibly reflecting their functions as remodelers of the stromal ECM. Indeed, several proteases are known to be made by both tumor cells and tumor-associated stromal cells (Breznik et al., 2017), and the presence of a protease in the stromal compartment does not preclude its manufacture, at least in part, by tumor cells. Therefore, we performed ISH to evaluate whether the mRNA that encodes each protease is α3β1 dependent within tumor cells. ISH was first performed using our tumorigenic TMKα3+ and TMKα3– lines (Figure 4). Each mRNA probe detected its target in an α3β1-dependent manner (Figure 4), consistent with our qPCR data (Figure 1a). ISH of skin tumors revealed that the levels of *Bmp1*, *Mmp9*, and *Mmp3* mRNAs were reduced in the tumor cells of epidermal α3β1-deficient papillomas tumors compared with those in the control tumors (Figure 5a and b). These data indicate that BMP-1, MMP-9, and MMP-3 are supplied, in large part, by the tumor cells in an integrin α3β1–dependent manner (Figure 5c).

Expression of *BMP1*, *MMP9*, and *MMP3* genes correlate with *ITGA3* gene expression in human SCC, and *ITGA3*, *BMP1*, and *MMP3* associate with poor survival outcome

Next, we used a bioinformatic approach (cBioPortal [Cerami et al., 2012; Gao et al., 2013]) to analyze the publicly available patient RNA-sequencing data (The Cancer Genome

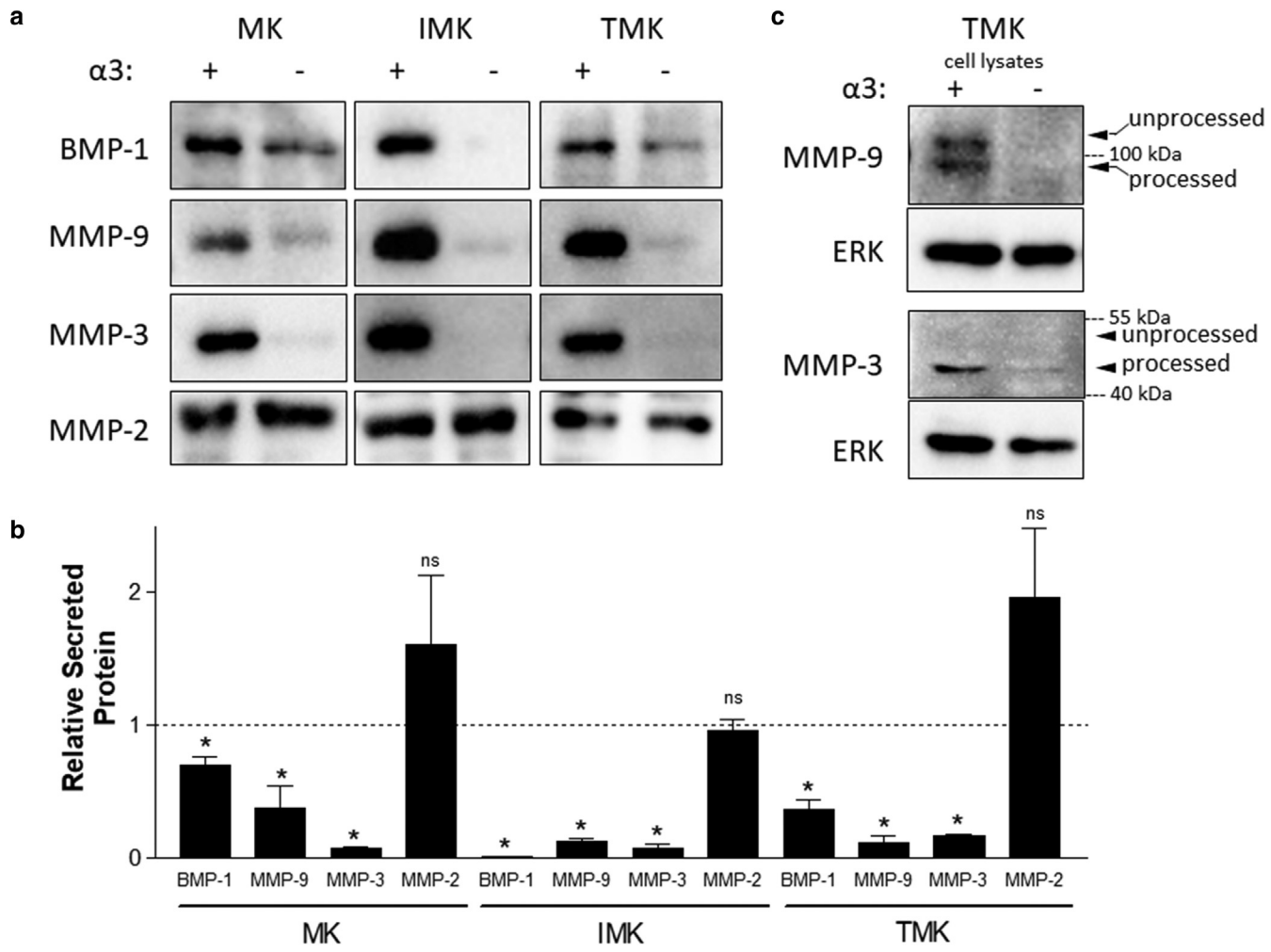

Figure 2. α3-Null cells have reduced BMP-1, MMP-9, and MMP-3 protein secretion. (**a, b**) Samples of conditioned medium were prepared from each keratinocyte line and analyzed by immunoblot for BMP-1, MMP-9, MMP-3, and MMP-2. (**a**) Representative immunoblots are shown. (**b**) The graph shows the quantification of immunoblots; bars represent the normalized secreted protein from α3-null cells, relative to those of their respective α3-expressing control (dotted line); n = 3. Data are presented as mean ± SEM; two-tailed *t*-test, $*P < 0.05$. (**c**) Whole-cell lysates from the TMK lines were isolated and then assayed by immunoblot for MMP-9 and MMP-3 or for total ERK as a loading control; the indicated bands for unprocessed and processed forms are consistent in size (kDa) with the reported sizes of mouse MMP-9 and MMP-3. ERK, extracellular signal–regulated kinase; IMK, immortalized mouse keratinocyte; MK, mouse keratinocyte; MMP, matrix metalloprotease; ns, nonsignificant; TMK, transformed mouse keratinocyte.

Atlas, PanCancer Atlas) to elucidate the relevance of our findings with human SCC. The analyzed dataset contains examples of human primary head and neck SCC from stages 1 to 4. Indeed, the expression of the *BMP1*, *MMP9,* and *MMP3* genes each correlated with the expression of the α3 subunit gene (i.e., *ITGA3*) in human SCC (Figure 6a), consistent with potential roles for BMP-1, MMP-9, and MMP-3 as downstream effectors of integrin α3β1. Furthermore, *ITGA3* gene expression is predictive of a poor outcome in human SCC, consistent with a protumorigenic role for α3β1 (Figure 6b). Importantly, *MMP3* gene expression also shows a significant association with poor survival in human SCC (Figure 6b). A trend toward the association of *BMP1* gene expression with poor survival in human SCC was observed but did not reach the 95% confidence interval (Figure 6b).

DISCUSSION

This study identifies epidermal integrin α3β1 as a regulator of several proteases within the secretome of skin tumor cells. We show that BMP-1, MMP-9, and MMP-3 are upregulated in an α3β1-dependent manner in a panel of three different immortalized and/or transformed KCs, two of which harbor genetic lesions that mimic common mutations in human SCC (Figures 1 and 2). This finding is consistent with the findings of our previous studies that identified the α3β1-dependent upregulation of BMP-1 and MMP-9 in different in vitro contexts (DiPersio et al., 2000; Iyer et al., 2005; Lamar et al., 2008; Longmate et al., 2018). Importantly, in this study, we show that this regulation is upheld in vivo where α3β1-deficient skin tumors display reduced levels of *Bmp1*, *Mmp9*, and *Mmp3* mRNA and secreted protein (Figures 3 and 5). Moreover, bioinformatic analyses suggest that *BMP1*, *MMP9,* and *MMP3* gene expression correlates with the expression of *ITGA3*, the gene that encodes the integrin α3 subunit, in human SCC (Figure 6a), supporting the clinical relevance of our murine models.

We have previously shown that the ablation of integrin α3β1 from established skin tumors, achieved through genetic

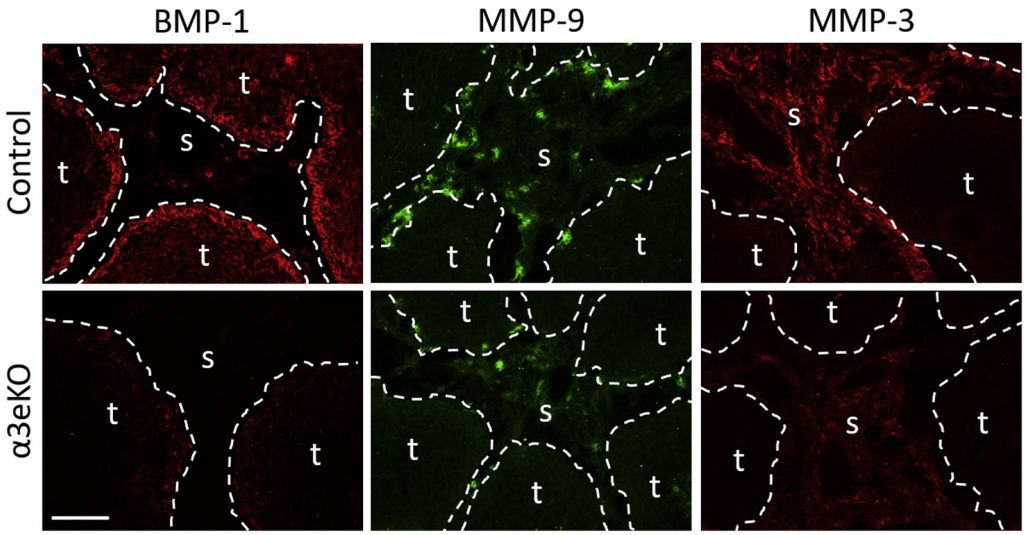

Figure 3. Integrin α3β1–deficient tumors display reduced levels of BMP-1, MMP-9, and MMP-3 protein. Tumor cryosections from control or α3eKO tumors were immunostained for BMP-1, MMP-9, and MMP-3. n ≥ 10 papillomas per group; The dashed line indicates the tumor–stroma boundary. Bar = 100 μm. For each protease, the distributions between the two groups differed significantly (Mann–Whitney *U* test: BMP-1 = 0, MMP-9 = 14, and MMP-3 = 8); $P < 0.01$, two-tailed. α3eKO, epidermal α3β1–deficient papillomas; MMP, matrix metalloprotease; s, stroma; t, tumor.

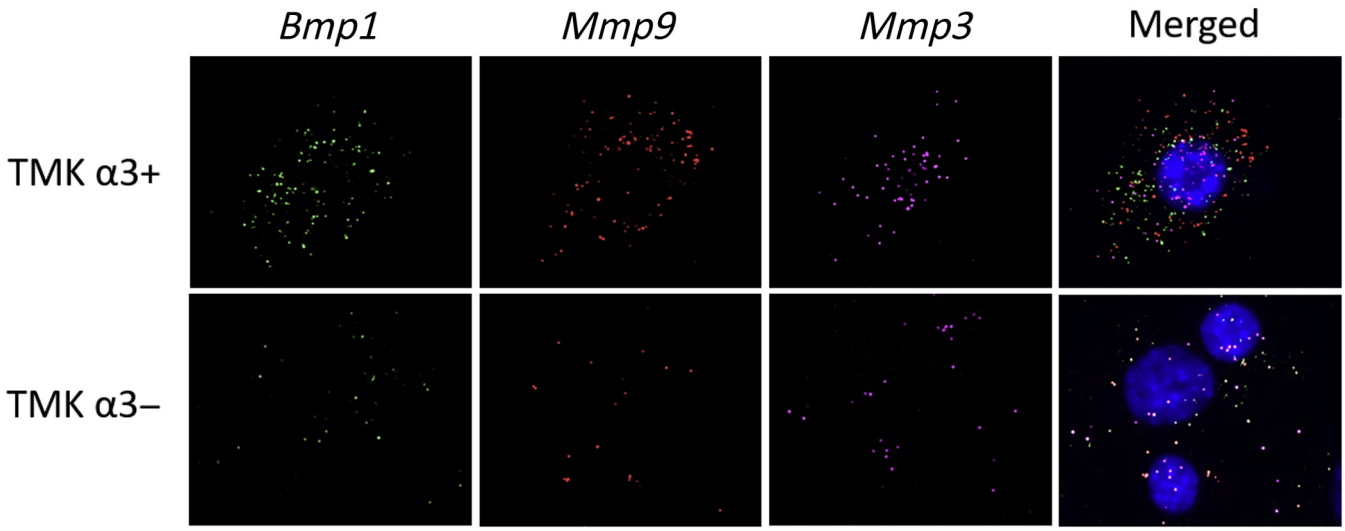

Figure 4. *Bmp1*, *Mmp9*, and *Mmp3* mRNA puncta are reduced in α3-null cells (TMK α3–) versus those in control cells (TMK α3+). ISH of cultured TMK cells was performed. Representative images are shown for *Bmp1* mRNA (green) and Mmp mRNAs, *Mmp9* (red) and *Mmp3* (purple). Merged images show *Bmp1* mRNA and MMP mRNAs, *Mmp9* and *Mmp3*, together with DAPI (blue) to mark the nuclei. ISH, in situ hybridization; MMP, matrix metalloprotease; TMK, transformed mouse keratinocyte.

deletion of the *Itga3* gene for the α3 subunit, leads to dramatic tumor regression in a murine model, indicating that α3β1 is protumorigenic (Longmate et al., 2021). Consistently, our current bioinformatic studies indicate that *ITGA3* gene expression is associated with poor survival in human SCC (Figure 6b). *MMP3* gene expression and to a lesser extent *BMP1* gene expression are also associated with poor survival in human SCC (Figure 6b), in accordance with these proteases being protumorigenic effectors downstream of α3β1. These findings are consistent with those of previous studies that have identified an association of poor survival with tumor cell expression of MMP-3 in pancreatic, pulmonary, and mammary carcinomas (Mehner et al., 2015) and with tumor cell expression of BMP-1 in clear cell renal cell carcinoma and gastric cancer (Rafi et al., 2021; Xiao et al., 2020).

Mechanistically, the α3β1-dependent regulation of BMP-1, MMP-9, and MMP-3 occurred at the level of mRNA expression, which was reflected in protein secretion. However, this does not preclude the possibility that α3β1 further regulates protease secretion through the exocytic process or as cargo within exosomes. Indeed, integrin-dependent signaling has been shown to coordinate exocytic machinery during the process of neurite sprouting in neurons (Gupton and Gertler, 2010), although it remains to be seen whether this is a general mechanism of secretome regulation by integrins in other contexts. Interestingly, integrins themselves are often found in

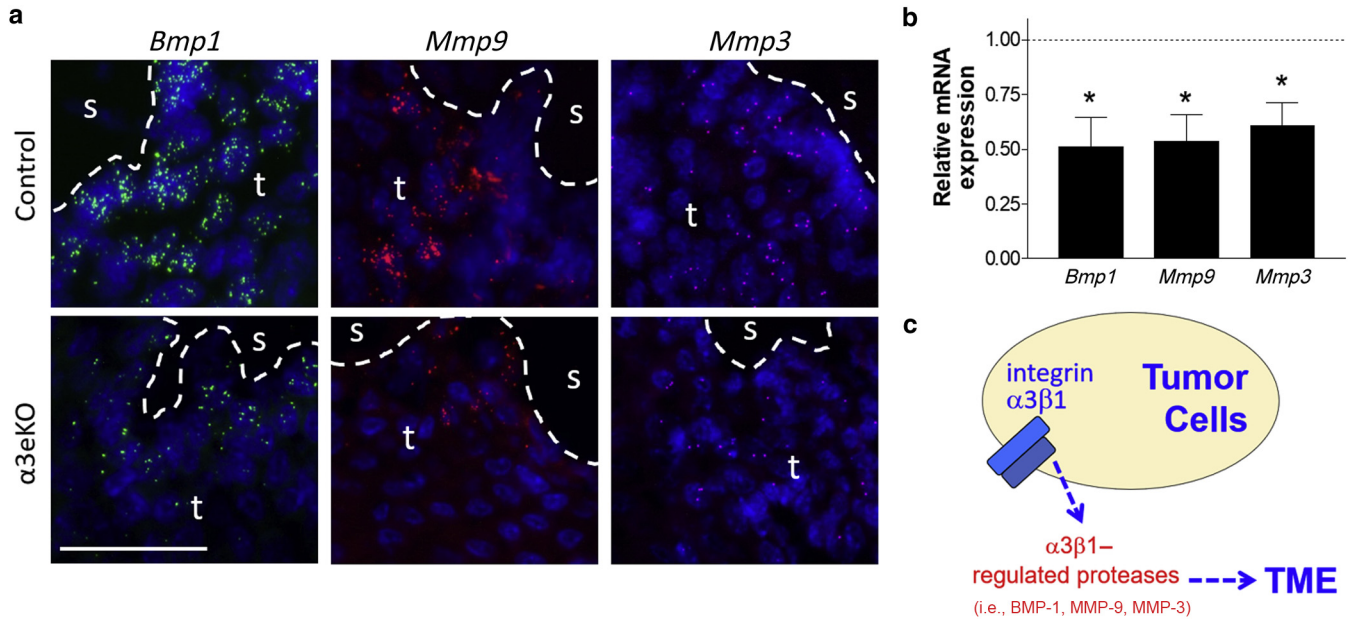

Figure 5. *Bmp1*, *Mmp9*, and *Mmp3* mRNAs are reduced in α3β1-deficient tumors. (**a, b**) ISH to detect mRNA was performed on tumor cryosections. (**a**) Representative images of tumor-derived *Bmp1* mRNA (green) and MMP mRNAs, *Mmp9* (red) and *Mmp3* (purple) from control and α3β1-deficient (α3eKO) tumors. The dashed line represents the tumor–stroma boundary. Bar = 50 μm. (**b**) Quantification of relative mRNA puncta in α3eKO tumors normalized to control (dotted line); n = 15 tumors per group. Mean ± SEM, two-tailed *t*-tests; $*P < 0.05$. (**c**) Model: α3β1 regulates the secreted proteases from tumor cells that alter the TME. α3eKO, epidermal α3β1–deficient papilloma; ISH, in situ hybridization; MMP, matrix metalloprotease; s, stroma; t, tumor; TME, tumor microenvironment.

exosome cargo, and exosome-derived integrins have been found to promote cancer progression (Fedele et al., 2015; Krishn et al., 2019; Paolillo and Schinelli, 2017). Furthermore, it is important to note that in two of the three KC lines, *Mmp2* mRNA was downregulated by α3β1. Although the level of protein secretion did not reach significance, it is important to note that some proteases may not be regulated by α3β1 or may be regulated differently.

Although this study indicates that metalloproteases are likely contributors of the integrin α3β1–dependent tumor growth, the exact roles for BMP-1, MMP-9, and MMP-3 in the growth and progression of cutaneous tumors remain to be delineated and are likely to be complex (Niland and Eble, 2020). MMPs, in general, are known to degrade ECM barriers and, by partial proteolysis, can also influence cells through the release of soluble ECM fragments called matrikines (Niland and Eble, 2020). Previous studies have identified a role for integrin-dependent MMP-9 in promoting the invasive capacity of epidermal tumor cells (Lamar et al., 2008; Thomas et al., 2001). Furthermore, BMP-1 suppression has been shown to inhibit the motility of gastric cancer cell lines (Hsieh et al., 2018), whereas MMP-3–ablated prostate tumors grew at a slower rate and were significantly less vascularized in an in vivo murine model (Frieling et al., 2020). In addition, it is possible that matrix degradation by these proteases allows for the release of GFs from the cell surface or matrix reservoirs allowing for enhanced tumor growth (Gill and Parks, 2008; Page-McCaw et al., 2007). In any case, it is likely that α3β1-dependent, tumor-derived proteases such as BMP-1, MMP-9, and MMP-3 promote tumor growth and progression through modifying the TME (Figure 5c).

Although this study has identified BMP-1, MMP-9, and MMP-3 as integrin α3β1–dependent, tumor-derived proteases (Figure 5c), extensive cross-talk to the TME indicates the possibility that these proteases may also be contributed by stromal cells in an epidermal α3β1-dependent manner. Indeed, we previously identified several important roles for epidermal α3β1 in the regulation of paracrine cross-talk to stromal cells. Examples include cross-talk from KCs to endothelial cells that promotes wound angiogenesis (Mitchell et al., 2009), cross-talk from KCs to fibroblasts that controls their differentiation state (Zheng et al., 2019), and cross-talk from epithelial tumor cells to tumor-associated macrophages to support their survival (Longmate et al., 2021). These so-called paracrine functions of α3β1 occur through the regulation of secreted factors, which can modulate the cross-talk to distinct cell types within the stroma or can impact matrix composition and remodeling. Furthermore, it has been shown that breast cancer cells induce the expression of MMP-9 by stromal fibroblasts through secreted factors, TNF-α and TGFβ (Stuelten et al., 2005).

The early identification of MMPs as critical regulators of cancer development and metastasis had indicated these proteases as potentially exciting therapeutic targets. However, broad-spectrum MMP inhibitors have historically produced disappointing results clinically, as reviewed (Winer et al., 2018). It is likely that more selective MMP inhibition that is targeted to specific MMPs that drive tumor progression, appropriate for the tumor type and stage, would produce better results with lower toxicity (Winer et al., 2018). It is intriguing to consider epithelial integrin α3β1 as a therapeutic target in the treatment of cancer because the pleiotropic effect of such targeting would inhibit several tumor-

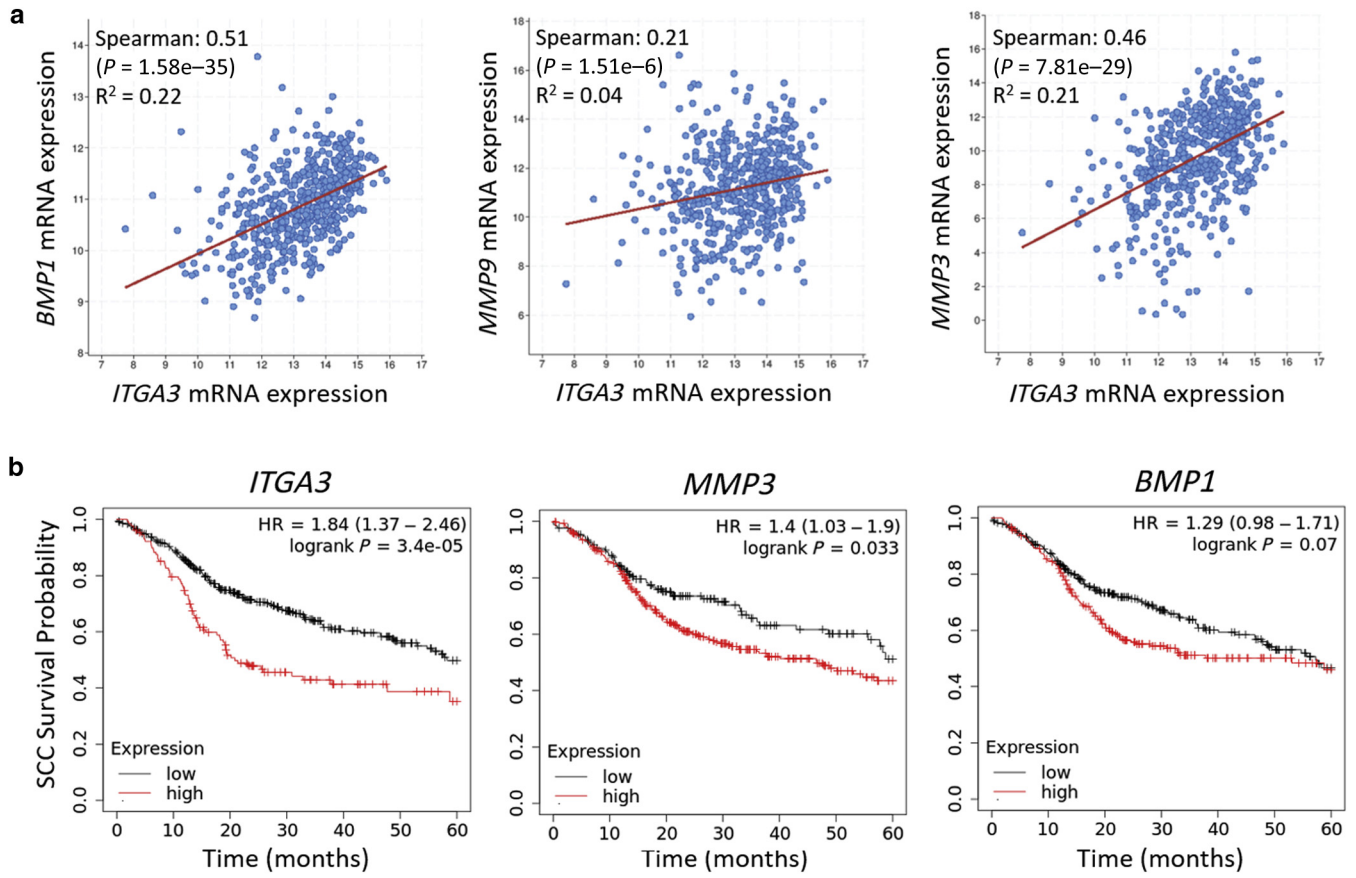

Figure 6. Expression of proteases correlates with *ITGA3* gene expression in human SCC, and *ITGA3* and *MMP3* associate with poor survival outcome. (**a**) Analysis of mRNA expression data from human patients with SCC shows a significant correlation of *ITGA3* expression with (left to right) *BMP1*, *MMP9*, and *MMP3* expression; Spearman correlation. Graphs were generated in cBioPortal. (**b**) KM plots showing a reduced overall survival probability of patients with high *ITGA3* or *MMP3* gene expression. A trend toward an association between poor survival outcome and high *BMP1* mRNA expression was observed, although this was not statistically significant. Graphs were generated using KM plotter. All analyses utilized the head and neck SCC dataset; TCGA, PanCancer Atlas. HR, hazard ratio; KM, Kaplan–Meier; MMP, matrix metalloprotease; SCC, squamous cell carcinoma; TCGA, The Cancer Genome Atlas.

promoting MMPs that could impact the microenvironment in a potentially powerful way. Recently, α3β1 has been exploited as a means of delivering targeted therapy to high α3-expressing human tumor xenografts in mice through a high-affinity and high-specificity peptide ligand called LXY30 (Zhang et al., 2021). Presumably, the efficacy of LXY30 would be further enhanced if the peptide could be modified to not only target α3β1 but to inhibit it. Although it is possible that systemic delivery of such treatment in humans may result in adverse events, topical application or local injection may be sufficient in the case of cutaneous SCC for efficacious targeting of α3β1.

Invariably, the successful utilization of integrin targets as a tool to mitigate tumor progression is complicated by the complexity of the TME. Moving forward, it will be important to further explore the efficacy of targeting integrin α3β1 on tumor cells while considering the potential effects on the secretome and the resulting impact on both the ECM and distinct cell types within the TME.

MATERIALS AND METHODS

MK lines

LTAg-immortalized MK cells (MKα3+ or MKα3–), p53-null IMK cells (IMKα3+ or IMKα3−), or RasV12-transformed variants of the latter lines (TMKα3+ or TMKα3−) that express or lack α3β1 were derived previously (Iyer et al., 2005; Lamar et al., 2008). Cells were cultured in MK growth medium as described (Lamar et al., 2008; Longmate et al., 2014; Missan et al., 2014). Cell lines are tested several times per year for mycoplasma using a PCR-based method (Young et al., 2010), and all in vitro studies were conducted within 6 months of the test date.

RNA isolation and qPCR

RNA from cultured cells was isolated using Trizol Reagent (Life Technologies, Waltham, MA) and DNase treated with Turbo DNA-free Kit (Ambion, Waltham, MA). cDNA was generated using the iScript cDNA Synthesis Kit (Bio-Rad, Hercules, CA). qPCR was performed using SsoAdvanced Universal SYBR Green Supermix (Bio-Rad) in the Bio-Rad CFX96 Touch thermocycler under the following conditions: (95 °C for 2 minutes) × 1 cycle; followed by (95 °C for 5 seconds and 60 °C for 30 seconds) × 39 cycles; melt curve analysis (65−95 °C, increment 0.5 °C for 5 seconds). The primer sequences for *BMP1* were forward: GACAACTCGGTACAGAGGAAAG and reverse: CGAACTGGGCATGGGAATAA. The primer sequences for *MMP9* were forward: CTGGAACTCACACGACATCTT and reverse: TCCACCTTGTTCACCTCATTT. The primer sequences for *MMP3* were forward: CAGGAAGATAGCTGAGGACTTTC and reverse: CTGCGAAGATCCACTGAAGAA.

The primer sequences for *MMP2* were forward: GCTCCACTCTTCTGGTTCTTC and reverse: CCCTCCTAAGCCAGTCTCTATTA. The primer sequences for *TBP* were forward: TGTATCTACCGTGAATCTTGGC and reverse: CCAGAACTGAAAATCAACGCAG. The primer sequences for *PPIA* were forward: CAAACACAAACGGTTCCCAG and reverse: TTCACCTTCCCAAAGACCAC. The primer sequences for *NONO* were forward: GGAGGTGCTATGGGCATAAA and reverse: GGTTCCATCTGGCATCATAGT. All the primers were purchased from IDT (Newark, NJ) and were designed using the IDT PrimerQuest tool. The geometric mean of three reference genes (*TBP*, *PPIA*, *NONO*) was used for normalization. Relative mRNA levels in α3− cells compared with those in their respective α3+ cells were calculated using the 2-(ΔΔCt) formula.

Preparation of CM

Cells were cultured in MK growth medium to ~80% confluence, then switched to serum-free medium, and cultured for another 24 hours. CM was collected, centrifuged for 3 minutes at $2 \times 10^3 g$ to remove cell debris, and concentrated using Amicon centrifugal filters with 3,000 molecular weight cut-off (Millipore, Darmstadt, Germany).

Immunoblot

Whole-cell lysates were prepared in nonreducing buffer (Cell Signaling Technology, Beverly, MA), and CM samples were prepared as described earlier. Protein concentrations were determined using the BCA Protein Assay kit (Pierce, Rockford, IL), and equal protein was resolved by 10% SDS-PAGE and assayed by immunoblot using the following antibodies at the indicated dilutions: anti–BMP-1 (1:200, Thermo Fisher Scientific, Rockford, IL), anti–MMP-3 (1:1,000, Abcam, Cambridge, MA); anti–MMP-9 (1:1,000, Abcam), anti–MMP-2 (1:1,000, Abcam), anti–α3 integrin subunit (1:1,000) (DiPersio et al., 1995), or anti–extracellular signal-regulated kinase (anti-ERK; 1:1,000, Santa Cruz Biotechnology, Santa Cruz, CA). The secondary antibodies used were horseradish peroxidase–conjugated goat anti-rabbit IgG (1:1,500, Cell Signaling Technology, Danvers, MA) or donkey anti-goat IgG (1:1,000, Santa Cruz Biotechnology), as appropriate. Chemiluminescence was performed using Super-Signal Kit (Pierce) and then was visualized using Bio-Rad ChemiDoc MP imaging system with Image Lab software (Bio-Rad).

Mouse studies

Details of K14CreERT:$\alpha3^{flx/flx}$ mice and two-step tumorigenesis experiments were supplied previously (Longmate et al., 2021, 2017). Briefly, topical treatment with 4-hydroxytamoxifen caused the deletion of floxed genes (Vasioukhin et al., 1999), generating confirmed epidermal α3β1-deficient papillomas, as detailed previously (Longmate et al., 2021). Vehicle-treated papillomas served as control. Tumors used in these studies were collected on treatment day 14 as described (Longmate et al., 2021). All animal experiments were approved by the Institutional Animal Care and Use Committee of Albany Medical College (Albany, NY).

Histology and immunostaining

Excised papillomas were embedded in optimal cutting temperature (Electron Microscopy Sciences, Hatfield, PA), and 6 μm cryosections were cut. Sections were used for in situ RNA detection (described in the following section) or immunostained as follows. Sections were rehydrated (0.02% Tween-20 and/or PBS) for 10 minutes, fixed (4% paraformaldehyde and/or 5% sucrose and/or PBS) for 10 minutes, permeabilized (0.4% TritonX-100 and/or PBS) for 10 minutes, blocked (3% BSA, 0.1% glycine, 0.1% Tween-20) for 30 minutes, blocked again (0.5% BSA, 10% goat serum, 0.1% Tween-20) for 30 minutes, and then stained with anti–MMP-3 (1:50, Abcam) or anti–MMP-9 (1:50, Abcam). Alternatively, sections were rehydrated (0.02% Tween-20 and/or PBS) for 10 minutes, fixed (4% paraformaldehyde and/or PBS) for 5 minutes, permeabilized (0.4% TritonX-100 and/or PBS) for 5 minutes, blocked (5% milk, 10% heat-inactivated goat serum, PBS) for 1 hour, and then stained with anti–BMP-1 (1:100, Abcam). Secondary antibodies (Molecular Probes, Eugene, OR) were Alexa Fluor 488 goat anti-rabbit IgG or Alexa Fluor 594 goat anti-rabbit IgG (1:250−1:500). Sections were costained with DAPI, mounted with ProLong Gold antifade mounting media (Molecular Probes), and imaged on a Nikon Eclipse 80i microscope (Tokyo, Japan) with a Photometrics Cool Snap ES camera (Tucson, AZ). Semiquantitative analysis of immunostaining was performed in a blinded fashion by assigning rank from least to most staining for each antibody and was then statistically analyzed using the Mann–Whitney *U* test.

In situ RNA detection

ISH was performed using the RNAScope Fluorescent Multiplex V1 kit (Advanced Cell Diagnostics, Newark, CA) on cultured cells or sections of fresh-frozen tumors (see the section discussed earlier). Cultured cells plated on collagen-coated coverslips were fixed in 4% paraformaldehyde for 30 minutes, dehydrated and rehydrated, and then digested with protease III for 10 minutes. Fresh-frozen tumor sections were fixed in 4% paraformaldehyde for 1 hour, dehydrated, and digested with protease IV for 22 minutes. After pretreatment, cells and tissue sections were incubated for 2 hours at 40 °C with probes to detect *BMP1* (311151), *MMP9* (472401-C2), or *MMP3* (480961-C3) mRNA, followed by wash and amplification steps according to the manufacturer's instructions. Sections were costained with DAPI, mounted with ProLong Gold antifade mounting media (Molecular Probes), and imaged on a Nikon Eclipse 80i microscope with a Photometrics Cool Snap ES camera. Image analysis was performed using Fiji ImageJ. Each image was individually thresholded (Otsu), and the number of mRNAs was counted using the analyze particles setting.

Bioinformatics

All bioinformatics analyses utilized patient data from the head and neck SCC data set generated by The Cancer Genome Atlas Research Network: https://www.cancer.gov/tcga. The data set contains 523 human samples from patients with primary head and neck SCC. Graphs were generated using CBioPortal (Cerami et al., 2012; Gao et al., 2013) or KM plotter (Nagy et al., 2021), as indicated.

Data availability statement

No datasets were generated during this study.

ORCIDs

Whitney M. Longmate: https://orcid.org/0000-0002-6514-7404
Rakshitha Pandulal Miskin: https://orcid.org/0000-0002-7200-4225
Livingston Van De Water: https://orcid.org/0000-0002-3825-9224
C. Michael DiPersio: https://orcid.org/0000-0001-9366-230X

AUTHOR CONTRIBUTIONS

Conceptualization: WML, CMD; Data Curation: WML, RPM; Formal Analysis: WML, RPM; Funding Acquisition: LVDW, CMD; Investigation: WML, RPM; Project Administration: LVDW, CMD; Resources: LVDW, CMD; Supervision: WML, RPM, CMD; Validation: WML, RPM; Visualization: WML, RPM; Writing - Original Draft Preparation: WML, RPM; Writing - Review and Editing: WML, RPM, LVDW, CMD

ACKNOWLEDGMENTS

This research was supported by the National Institutes of Health grants from the National Institute of Arthritis and Musculoskeletal Skin Disease to CMD and LVDW (R01AR063778) and from the National Cancer Institute to CMD (R01CA129637). We thank Christina Nickerson (Albany Medical Center Histology Core) for tissue sectioning and Scott Varney for technical assistance.

CONFLICT OF INTEREST

The authors state no conflict of interest.

REFERENCES

Abel EL, Angel JM, Kiguchi K, DiGiovanni J. Multi-stage chemical carcinogenesis in mouse skin: fundamentals and applications. Nat Protoc 2009;4:1350–62.

Bonnans C, Chou J, Werb Z. Remodelling the extracellular matrix in development and disease. Nat Rev Mol Cell Biol 2014;15:786–801.

Breznik B, Motaln H, Lah Turnšek T. Proteases and cytokines as mediators of interactions between cancer and stromal cells in tumours. Biol Chem 2017;398:709–19.

Cerami E, Gao J, Dogrusoz U, Gross BE, Sumer SO, Aksoy BA, et al. The cBio cancer genomics portal: an open platform for exploring multidimensional cancer genomics data [published correction appears in Cancer Discov 2012;2:960]. Cancer Discov 2012;2:401–4.

Cooper J, Giancotti FG. Integrin signaling in cancer: mechanotransduction, stemness, epithelial plasticity, and therapeutic resistance. Cancer Cell 2019;35:347–67.

De Groef L, Andries L, Lemmens K, Van Hove I, Moons L. Matrix metalloproteinases in the mouse retina: a comparative study of expression patterns and MMP antibodies. BMC Ophthalmol 2015;15:187.

DiPersio CM, Shah S, Hynes RO. Alpha 3A beta 1 integrin localizes to focal contacts in response to diverse extracellular matrix proteins. J Cell Sci 1995;108:2321–36.

DiPersio CM, Shao M, Di Costanzo L, Kreidberg JA, Hynes RO. Mouse keratinocytes immortalized with large T antigen acquire alpha3beta1 integrin-dependent secretion of MMP-9/gelatinase B. J Cell Sci 2000;113:2909–21.

Fedele C, Singh A, Zerlanko BJ, Iozzo RV, Languino LR. The αvβ6 integrin is transferred intercellularly via exosomes. J Biol Chem 2015;290:4545–51.

Flores-Reséndiz D, Castellanos-Juárez E, Benítez-Bribiesca L. [Proteases in cancer progression]. Gac Med Mex 2009;145:131–42 [in Spanish].

Frieling JS, Li T, Tauro M, Lynch CC. Prostate cancer-derived MMP-3 controls intrinsic cell growth and extrinsic angiogenesis. Neoplasia 2020;22:511–21.

Gao J, Aksoy BA, Dogrusoz U, Dresdner G, Gross B, Sumer SO, et al. Integrative analysis of complex cancer genomics and clinical profiles using the cBioPortal. Sci Signal 2013;6:pl1.

Gill SE, Parks WC. Metalloproteinases and their inhibitors: regulators of wound healing. Int J Biochem Cell Biol 2008;40:1334–47.

Goździalska A, Wojas-Pelc A, Drąg J, Brzewski P, Jaśkiewicz J, Pastuszczak M. Expression of metalloproteinases (MMP-2 and MMP-9) in basal-cell carcinoma. Mol Biol Rep 2016;43:1027–33.

Gupton SL, Gertler FB. Integrin signaling switches the cytoskeletal and exocytic machinery that drives neuritogenesis. Dev Cell 2010;18:725–36.

Hamidi H, Ivaska J. Every step of the way: integrins in cancer progression and metastasis [published correction appears in Nat Rev Cancer 2019;19:179]. Nat Rev Cancer 2018;18:533–48.

He Y, Thriene K, Boerries M, Hausser I, Franzke CW, Busch H, et al. Constitutional absence of epithelial integrin α3 impacts the composition of the cellular microenvironment of ILNEB keratinocytes. Matrix Biol 2018;74:62–76.

Hsieh YY, Tung SY, Pan HY, Yen CW, Xu HW, Deng YF, et al. Upregulation of bone morphogenetic protein 1 is associated with poor prognosis of late-stage gastric cancer patients. BMC Cancer 2018;18:508.

Hynes RO. Integrins: bidirectional, allosteric signaling machines. Cell 2002;110:673–87.

Iyer V, Pumiglia K, DiPersio CM. Alpha3beta1 integrin regulates MMP-9 mRNA stability in immortalized keratinocytes: a novel mechanism of integrin-mediated MMP gene expression. J Cell Sci 2005;118:1185–95.

Krishn SR, Singh A, Bowler N, Duffy AN, Friedman A, Fedele C, et al. Prostate cancer sheds the αvβ3 integrin in vivo through exosomes. Matrix Biol 2019;77:41–57.

Lamar JM, Pumiglia KM, DiPersio CM. An immortalization-dependent switch in integrin function up-regulates MMP-9 to enhance tumor cell invasion. Cancer Res 2008;68:7371–9.

Longmate WM. Keeping a secretome: emerging roles for epithelial integrins in controlling a stroma-supportive secretome. J Dermatol Skin Sci 2020;2:13–20.

Longmate WM, Lyons SP, Chittur SV, Pumiglia KM, Van De Water L, DiPersio CM. Suppression of integrin α3β1 by α9β1 in the epidermis controls the paracrine resolution of wound angiogenesis. J Cell Biol 2017;216:1473–88.

Longmate WM, Lyons SP, DeFreest L, Van De Water L, DiPersio CM. Opposing roles of epidermal integrins α3β1 and α9β1 in regulation of mTLD/BMP-1-mediated laminin-γ2 processing during wound healing. J Invest Dermatol 2018;138:444–51.

Longmate WM, Monichan R, Chu ML, Tsuda T, Mahoney MG, DiPersio CM. Reduced fibulin-2 contributes to loss of basement membrane integrity and skin blistering in mice lacking integrin α3β1 in the epidermis. J Invest Dermatol 2014;134:1609–17.

Longmate WM, Varney S, Power D, Miskin RP, Anderson KE, DeFreest L, et al. Integrin α3β1 on tumor keratinocytes is essential to maintain tumor growth and promotes a tumor-supportive keratinocyte secretome. J Invest Dermatol 2021;141:142–51.e6.

Mehner C, Miller E, Nassar A, Bamlet WR, Radisky ES, Radisky DC. Tumor cell expression of MMP3 as a prognostic factor for poor survival in pancreatic, pulmonary, and mammary carcinoma. Genes Cancer 2015;6:480–9.

Missan DS, Chittur SV, DiPersio CM. Regulation of fibulin-2 gene expression by integrin α3β1 contributes to the invasive phenotype of transformed keratinocytes. J Invest Dermatol 2014;134:2418–27.

Mitchell K, Szekeres C, Milano V, Svenson KB, Nilsen-Hamilton M, Kreidberg JA, et al. Alpha3beta1 integrin in epidermis promotes wound angiogenesis and keratinocyte-to-endothelial-cell crosstalk through the induction of MRP3. J Cell Sci 2009;122:1778–87.

Nagy Á, Munkácsy G, Győrffy B. Pancancer survival analysis of cancer hallmark genes. Sci Rep 2021;11:6047.

Niland S, Eble JA. Hold on or cut? Integrin- and MMP-mediated cell-matrix interactions in the tumor microenvironment. Int J Mol Sci 2020;22:238.

Page-McCaw A, Ewald AJ, Werb Z. Matrix metalloproteinases and the regulation of tissue remodelling. Nat Rev Mol Cell Biol 2007;8:221–33.

Paolillo M, Schinelli S. Integrins and exosomes, a dangerous liaison in cancer progression. Cancers (Basel) 2017;9:95.

Rafi JH, Jafar T, Pathan MT, Reza R, Islam S, Sourna IJ, et al. High expression of bone morphogenetic protein 1 (BMP1) is associated with a poor survival rate in human gastric cancer, a dataset approaches. Genomics 2021;113:1141–54.

Ramovs V, Krotenberg Garcia A, Song JY, de Rink I, Kreft M, Goldschmeding R, et al. Integrin α3β1 in hair bulge stem cells modulates CCN2 expression and promotes skin tumorigenesis. Life Sci Alliance 2020;3:e202000645.

Ruokolainen H, Pääkkö P, Turpeenniemi-Hujanen T. Expression of matrix metalloproteinase-9 in head and neck squamous cell carcinoma: a potential marker for prognosis. Clin Cancer Res 2004;10:3110–6.

Sachs N, Secades P, van Hulst L, Kreft M, Song JY, Sonnenberg A. Loss of integrin α3 prevents skin tumor formation by promoting epidermal turnover and depletion of slow-cycling cells. Proc Natl Acad Sci USA 2012;109:21468–73.

Stuelten CH, DaCosta Byfield S, Arany PR, Karpova TS, Stetler-Stevenson WG, Roberts AB. Breast cancer cells induce stromal fibroblasts to express MMP-9 via secretion of TNF-alpha and TGF-beta. J Cell Sci 2005;118:2143–53.

Subbaram S, DiPersio CM. Integrin α3β1 as a breast cancer target. Expert Opin Ther Targets 2011;15:1197–210.

Thomas GJ, Lewis MP, Hart IR, Marshall JF, Speight PM. AlphaVbeta6 integrin promotes invasion of squamous carcinoma cells through up-regulation of matrix metalloproteinase-9. Int J Cancer 2001;92:641–50.

Vasioukhin V, Degenstein L, Wise B, Fuchs E. The magical touch: genome targeting in epidermal stem cells induced by tamoxifen application to mouse skin. Proc Natl Acad Sci USA 1999;96:8551–6.

White AC, Tran K, Khuu J, Dang C, Cui Y, Binder SW, et al. Defining the origins of Ras/p53-mediated squamous cell carcinoma. Proc Natl Acad Sci USA 2011;108:7425–30.

Winer A, Adams S, Mignatti P. Matrix metalloproteinase inhibitors in cancer therapy: turning past failures into future successes. Mol Cancer Ther 2018;17:1147–55.

Xiao W, Wang X, Wang T, Xing J. Overexpression of BMP1 reflects poor prognosis in clear cell renal cell carcinoma. Cancer Gene Ther 2020;27:330–40.

Young L, Sung J, Stacey G, Masters JR. Detection of mycoplasma in cell cultures. Nat Protoc 2010;5:929–34.

Zhang L, Wu Y, Yin X, Zhu Z, Rojalin T, Xiao W, et al. Tumor receptor-mediated in vivo modulation of the morphology, phototherapeutic properties, and pharmacokinetics of smart nanomaterials. ACS Nano 2021;15:468–79.

Zheng R, Longmate WM, DeFreest L, Varney S, Wu L, DiPersio CM, et al. Keratinocyte integrin α3β1 promotes secretion of IL-1α to effect paracrine regulation of fibroblast gene expression and differentiation. J Invest Dermatol 2019;139:2029–38.e3.